

# ChemComm

Accepted Manuscript



This article can be cited before page numbers have been issued, to do this please use: W. Chen, Y. Yuan, Z. ZHU, S. Ni, Z. Jiang, L. Liao, F. WONG and C. Lee, *Chem. Commun.*, 2018, DOI: 10.1039/C8CC00903A.



This is an Accepted Manuscript, which has been through the Royal Society of Chemistry peer review process and has been accepted for publication.

Accepted Manuscripts are published online shortly after acceptance, before technical editing, formatting and proof reading. Using this free service, authors can make their results available to the community, in citable form, before we publish the edited article. We will replace this Accepted Manuscript with the edited and formatted Advance Article as soon as it is available.

You can find more information about Accepted Manuscripts in the [author guidelines](#).

Please note that technical editing may introduce minor changes to the text and/or graphics, which may alter content. The journal's standard [Terms & Conditions](#) and the ethical guidelines, outlined in our [author and reviewer resource centre](#), still apply. In no event shall the Royal Society of Chemistry be held responsible for any errors or omissions in this Accepted Manuscript or any consequences arising from the use of any information it contains.

## A novel spiro-annulated benzimidazole host for highly efficient blue phosphorescent organic light-emitting devices

Wen-Cheng Chen,<sup>a</sup> Yi Yuan,<sup>b</sup> Ze-Lin Zhu,<sup>a</sup> Shao-Fei Ni,<sup>c</sup> Zuo-Quan Jiang,<sup>b</sup> Liang-Sheng Liao,<sup>\*b</sup> Fu-Lung Wong<sup>a</sup> and Chun-Sing Lee<sup>\*a</sup>

Received 00th January 20xx,  
Accepted 00th January 20xx

DOI: 10.1039/x0xx00000x

www.rsc.org/chemcomm

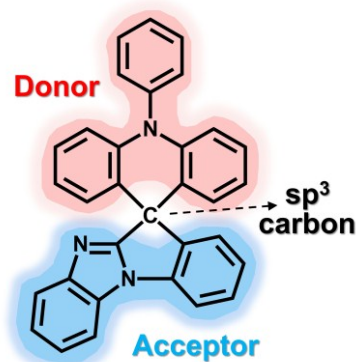
**A novel host material featuring spiro-annulated benzimidazole configuration is exploited for blue phosphorescent organic light-emitting devices (PhOLEDs). The new material exhibits a high triplet energy (3.07 eV) and a bipolar characteristic, and is effective as the host for Firpic-, Flr6- and FK306-based blue PhOLEDs with high performances.**

Phosphorescent organic light-emitting devices (PhOLEDs) employing noble metal complexes as emitting cores have received tremendous attention, because they can fully utilize both singlet and triplet excitons for radiation.<sup>1,2</sup> To date, high-performance sky-blue, green and red PhOLEDs have been widely used. Nevertheless, effective pure-blue or even deep-blue PhOLEDs have not been realized, mainly due to the lack of reliable host materials.<sup>3</sup>

Generally, in a PhOLED the emissive phosphors are dispersed in host materials to alleviate triplet exciton quenching via triplet-triplet annihilation (TTA).<sup>4</sup> To realize high-performance blue PhOLEDs, the host material is required to have (i) suitable highest occupied molecular orbital (HOMO) and lowest unoccupied molecular orbital (LUMO) levels for efficient hole and electron injection, (ii) bipolar electrical property for ensuring a wide carrier recombination zone, (iii) a high enough first triplet energy level ( $E_T$ ) to sensitize the blue phosphorescent dopant and to minimize energy leak and (iv) high enough thermal stability for thermal evaporation and against Joule heat during device operation. Molecules with spiro-core are promising candidates in constructing bipolar host

materials with high  $E_T$ s due to their intrinsic non-conjugated orthogonal configuration.<sup>5,6</sup> The stereo molecular configuration also endows spiro-based organic semiconductors with good thermal properties. The  $sp^3$ -hybridized spiro carbon atom separates the molecule into two moieties, so that electron donor and acceptor can be respectively incorporated to the two molecular halves for bipolar nature without lowering the  $E_T$  markedly.<sup>7</sup> However, this strategy is still hard to obtain bipolar host materials with very high  $E_T$ s, which are limited by the inherent conjugation of the incorporated electron donor or acceptor groups.

In this work, we report a novel bipolar host with a high  $E_T$  by tactfully incorporating a triphenylamine (TPA) moiety to a novel spiro-configured benzimidazole (BI) scaffold via a non-conjugated linking style (Scheme 1). BI was often used as an efficient electron-transporting building block in host materials for blue PhOLEDs.<sup>8,9</sup> The number 2 carbon atom (C2) of BI is jointed to the spiro carbon, while a benzene ring is simultaneously attached to the pyrrole-like nitrogen of BI and spiro carbon with an  $sp^3$  linkage, forming a rigid non-conjugated triangular configuration. This special donor-spiro-acceptor design endows the resulting material SPBI-TPA with a bipolar



Scheme 1 Chemical structure of SPBI-TPA.

<sup>a</sup> Center of Super-Diamond and Advanced Films (COSDAF) and Department of Chemistry, City University of Hong Kong, Hong Kong SAR, PR China. E-mail: apcslee@cityu.edu.hk

<sup>b</sup> Jiangsu Key Laboratory for Carbon-Based Functional Materials & Devices, Institute of Functional Nano & Soft Materials (FUNSOM) & Collaborative Innovation Center of Suzhou Nano Science and Technology, Soochow University, Suzhou, 215123, PR China. E-mail: lsiao@suda.edu.cn

<sup>c</sup> Department of Chemistry, Southern University of Science and Technology, Shenzhen, 518055, PR China

† Electronic Supplementary Information (ESI) available: See DOI: 10.1039/x0xx00000x

nature and a high  $E_T$  of 3.07 eV, which is higher than most of the fluorene-spiro-annulated compounds.<sup>5,6,10,11</sup> SPBI-TPA is effective as a host for Flrpic-, Flr6- and FK306-based blue PhOLEDs with high performances, which outperform its fluorene-based counterpart. This study presents the first example of spiro-annulated BI compound and provides a promising molecular template on the evolution of highly efficient host materials with high  $E_T$ s.

SPBI-TPA was prepared by a facile three-step procedure as shown in Scheme S1, and its detailed synthesis is shown in the ESI†. The key intermediate 11*H*-benzo[4,5]imidazo[1,2-*a*]indol-11-one (BIO)<sup>12</sup> was synthesized via a base-catalyzed cyclization reaction involving 2-fluorobenzaldehyde and 1*H*-benzo[*d*]imidazole under an atmosphere condition. Then BIO was reacted to lithium activated 2-bromo-*N,N*-diphenylaniline to afford an alcohol compound (hard to dissolve in common solvents, not isolated), followed by an intramolecular cyclization in an acidic condition to obtain the final product. To study the effects of using the BI-based spiro ring instead of the commonly used fluorene-based spiro system, a corresponding fluorene-based compound SPF-TPA (Scheme S2) was also synthesized.

Calculated molecular configuration of SPBI-TPA is shown in Fig. 1. Similar to the SPF-TPA (Fig. S1) and other reported fluorene-based spiro compounds,<sup>5,6</sup> the 1-phenyl-1*H*-benzo[*d*]imidazole section and the TPA fragments are perpendicular to each other, showing a high twisting angle of 87°. This orthogonal geometry is conducive to confining  $\pi$  conjugation and enhancing morphological stability.<sup>13</sup> Interestingly, TPA moiety in the molecule also displays a bend configuration (marked with a red arrow in Fig. 1), possibly stemming from the intramolecular interaction between the pyridine-like nitrogen atom of BI (N3) and the hydrogen atom of phenyl group in TPA (Fig. 1). As expected, the HOMO distribution is mainly located on the TPA fragment, while the 1-

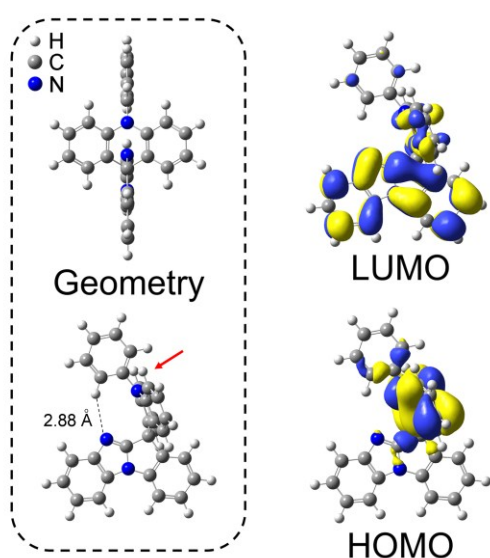


**Fig. 1** Calculated molecular geometry and frontier molecular orbital distribution of SPBI-TPA.

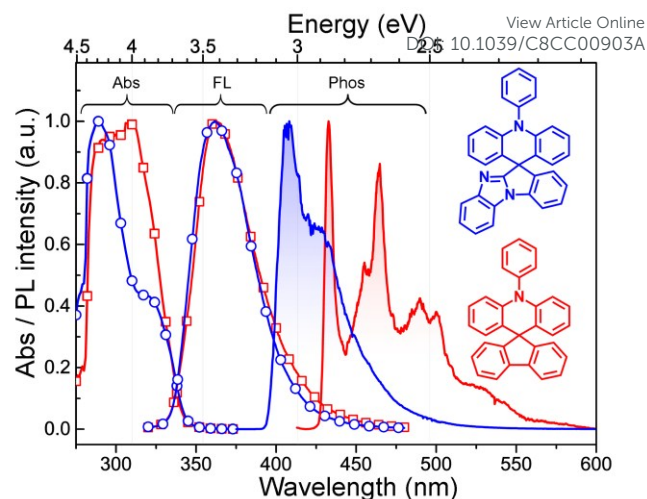


**Fig. 2** Absorption (Abs), fluorescence (FL) and phosphorescence (Phos) spectra of SPBI-TPA and SPF-TPA.

phenyl-1*H*-benzo[*d*]imidazole segment dominates the LUMO, implying a potential bipolar characteristic.

Thermal properties of the SPBI-TPA and SPF-TPA were studied using thermogravimetric analyzer (TGA) and differential scanning calorimetry (DSC). Benefited from the rigid and bulky spiro-configured BI scaffold, SPBI-TPA has a considerably higher decomposition temperature of 315 °C ( $T_d$ , 5% weight loss) comparing to that (285 °C) of SPF-TPA (Fig. S2, ESI†). Due to the bulky and rigid 3D molecular configuration by virtue of the orthogonal molecular structure, no evident glass transition temperatures ( $T_g$ s) are observed in SPBI-TPA and SPF-TPA (inset of Fig. S2, ESI†), demonstrating good thermal properties.

The absorption and fluorescence (FL) spectra in toluene solution are displayed in Fig. 2. The ~290-nm absorption bands can be attributed to the  $n\text{-}\pi^*$  transition of the TPA, which are similar to the previous reports,<sup>14,15</sup> and this is also in accord with the  $S_0 \rightarrow S_1$  natural transition orbital (NTO) analyses (Fig. S3, ESI†).<sup>16</sup> In addition, the NTO analyses suggested that the longer-wavelength absorption bands may involve ICT absorptions (From TPA to BI or fluorene). From the absorption onset of the solid thin films (Fig. S4, ESI†), the optical energy gaps ( $E_g$ s) of SPBI-TPA and SPF-TPA are estimated to be 3.52 and 3.41 eV, respectively. Combined with the HOMO levels measured with cyclic voltammetry (Fig. S5, ESI†), which are respectively estimated to be -5.40 and -5.29 eV for SPBI-TPA and SPF-TPA, LUMO levels of the two compounds are both estimated to be -1.88 eV. Both compounds show similar PL profiles with violet-blue emissions peaking at 361 and 362 nm for SPBI-TPA and SPF-TPA, respectively. Fig. 2 also shows the phosphorescence (Phos) spectra in 2-methyl-THF matrix at 77 K. It is obvious that SPBI-TPA shows a much shorter-wavelength Phos comparing to that of SPF-TPA.  $E_T$ s are determined to be 3.07 and 2.86 eV for SPBI-TPA and SPF-TPA, respectively. Fig. S6 in the ESI† shows the spin density distribution (SDD) in  $T_1$  states of SPBI-TPA and SPF-TPA. It is found that the SDD of SPF-TPA mainly localized on fluorene, the fragment with the highest degree of molecular conjugation. By contrast, the SDD of SPBI-TPA is mainly concentrated on the segment of the spiro-annulated TPA with a minor contribution

**Table 1** EL performances of the fabricated PhOLEDs

Host	Dopant	$V_{on}^a$ (V)	Max efficiency <sup>b</sup> ( $cd\ A^{-1}/\%$ )	CIE ( $x, y$ ) <sup>c</sup>
SPBI-TPA	Firpic	2.9	$55.1 \pm 0.7/25.5 \pm 0.3$	(0.17, 0.34)
SPBI-TPA	Fir6	3.1	$38.9 \pm 0.7/24.1 \pm 0.4$	(0.16, 0.25)
SPBI-TPA	FK306	2.9	$32.1 \pm 0.4/20.9 \pm 0.3$	(0.16, 0.20)
SPF-TPA	Firpic	3.0	$33.4 \pm 0.8/16.6 \pm 0.5$	(0.16, 0.33)
SPF-TPA	FK306	3.4	$10.5 \pm 1.1/6.8 \pm 0.7$	(0.16, 0.20)

<sup>a</sup> Turn-on voltage (detected at  $1\ cd\ m^{-2}$ ). <sup>b</sup> Current efficiency and external quantum efficiency at maximum. <sup>c</sup> Obtained at  $100\ cd\ m^{-2}$ .

from the BI moiety, which may be the reason for its relatively high  $E_T$ . It is worth pointing out that the  $E_T$  of SPBI-TPA is among the highest values of the spiro-based host materials.<sup>5,6,10,11</sup> We also compare the PL spectra of the present spiro-configured SPBI-TPA with a reported single bond connecting molecule BI-TPA<sup>17</sup> in different solvents, as shown in Fig. S7 (ESI<sup>†</sup>). Upon solvent polarity increases, the PL spectra of SPBI-TPA only show a mild red shift, and their spectral profiles remain almost unchanged. On the other hand, BI-TPA demonstrates significant red shifts in emission as medium polarity raises, showing a broad and structureless PL spectrum in acetonitrile ( $\lambda_{PL} = 439\ nm$  versus  $385\ nm$  in hexane). This suggests that the spiro-linking style can effectively suppress intramolecular charge transfer (ICT) interaction between the electron donor (TPA) and acceptor (BI), and thus ensuring a high  $E_T$ .

Hole-only and electron-only devices (HODs and EODs) using SPBI-TPA and SPF-TPA were fabricated and their current density-voltage ( $J$ - $V$ ) characteristics are shown in Fig. S8 (ESI<sup>†</sup>). Both compounds show high hole conductivity, which are original from the TPA donor. Because the HOMO offset between SPBI-TPA and SPF-TPA is not large ( $\sim 0.1\ eV$ ), and both materials have negligible hole-injection barrier to NPB ( $\sim 5.40\ eV$ ). Thus, the much higher hole current in the HOD based on SPF-TPA indicates that SPF-TPA has a better hole-transporting property than that of SPBI-TPA, mainly due to the better  $\pi$  conjugation of fluorene. On the other hand, even though SPBI-TPA and SPF-TPA have the same LUMO levels, the SPBI-TPA based EOD

displays much higher electron current. The better electron-transporting property can be attributed to the azo-BI segment, which may facilitate intermolecular electron hopping in solid state.<sup>18</sup> The employment of BI in the spiro system can simultaneously enhance the electron-transporting property and increase the  $E_T$ , which are beneficial for designing high-performance host for blue PhOLEDs.

To study the electroluminescence (EL) characteristics of SPBI-TPA as a host, a series of blue PhOLEDs were fabricated with a structure of ITO/1,4,5,8,9,11-hexaazatriphenylene-hexacarbonitrile (HAT-CN,  $10\ nm$ )/1,1-bis[4-[*N,N*-di(*p*-tolyl)amino]phenyl]cyclohexane (TAPC,  $50\ nm$ )/4,4',4''-tris(carbazol-9-yl)triphenylamine (TCTA,  $10\ nm$ )/SPBI-TPA: 10 wt% blue phosphor (20 nm)/1,3,5-tri[(3-pyridyl)-phen-3-yl]benzene (TmPyPB,  $40\ nm$ )/LiF ( $1\ nm$ )/Al ( $150\ nm$ ). Firpic, Fir6 and FK306<sup>19</sup> with  $E_T$ s of 2.62, 2.73 and 2.83 eV, respectively, are employed as the emissive dopants. The key device performance parameters are listed in Table 1. All the SPBI-TPA based devices show low turn-on voltage ( $V_{on}$ , at  $1\ cd\ m^{-2}$ ) at around 3 V. The SPBI-TPA hosted Firpic PhOLED emits a sky-blue EL emission with Commission Internationale de l'Éclairage (CIE) coordinates of (0.17, 0.34) (Fig. 3a), and has a respectable external quantum efficiency (EQE) of 25.5% at maximum (Fig. 3b), which outperform the corresponding device with the SPF-TPA host (EQE<sub>max</sub> = 16.6%, Fig. S9 in the ESI<sup>†</sup>). Besides the high  $E_T$ , the more balanced hole/electron-transporting properties are also responsible for the higher efficiency in the SPBI-TPA based PhOLED. Because the use of bipolar SPBI-TPA as a host can avoid recombination zone shifting towards the neighboring layers for a better charge utilization. Upon changing the dopant to Fir6 and FK306, the EL spectra shift towards shorter wavelength region (Fig. 3a), demonstrating deeper blue color indexes of (0.16, 0.25) and (0.16, 0.20), respectively, which are similar to those in literature.<sup>19,20</sup> It is worth noting that the Fir6 and the FK306 based PhOLEDs employing SPBI-TPA as host exhibit decent performances with maximum EQEs higher than 20%. By contrast, the FK306 based PhOLED using SPF-TPA as the host has a low performance, with an EQE<sub>max</sub> of only 6.8% (Fig. S9). The inferior efficiency of the SPF-TPA hosted FK306-based PhOLED is due to the comparable  $E_T$  of the host (2.86 eV) and the dopant (2.83 eV); the triplet excitons cannot be effectively confined within the dopant molecules. To the best of our knowledge, the performances of the devices employing SPBI-TPA as host are comparable to those of corresponding state-of-the-art PhOLEDs with respectively Firpic,<sup>21</sup> Fir6<sup>22</sup> and FK306<sup>19</sup> dopants.

In summary, a spiro-configured BI compound is designed and synthesized for the first time. The unique triangular configuration among BI, benzene (N1 substituted to BI) and TPA fragments is established via a spiro carbon atom, resulting in a short-conjugation compound SPBI-TPA with a high  $E_T$  of 3.07 eV. SPBI-TPA is demonstrated to have better thermal properties, a higher  $E_T$  and more balanced charge transportation than its fluorene counterpart. SPBI-TPA is effectively used as host for Firpic, Fir6 and FK306 based PhOLEDs, showing respectable EQEs over 20%. This work provides a novel host design strategy for high-performance blue PhOLEDs. In fact, the present BI-

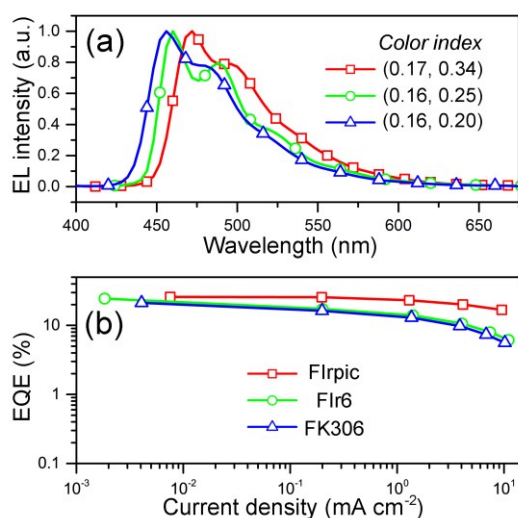


**Fig. 3** (a) EL spectra and (b) EQE-current density curves of the PhOLEDs using SPBI-TPA as host.

configured spiro system offers an isolated phenyl group (N1 substituted to BI) for modifying. We also believe that substituting electron-withdrawing moiety to this phenyl group via a facile approach<sup>23</sup> can further deepen the LUMO level without greatly lowering  $E_T$ , which should be a promising host system for thermally activated delayed fluorescence dopants with generally deep HOMO and LUMO levels.

We would like to acknowledge the financial support from the National Key R&D Program of China (Project No.: 2016YFB0401002), and Natural Science Foundation of China (Project Nos. 61575136 and 21572152).

## Notes and references

- 1 M. A. Baldo, D. F. O'Brien, Y. You, A. Shoustikov, S. Sibley, M. E. Thompson and S. R. Forrest, *Nature*, 1998, **395**, 151–154.
- 2 C. Adachi, M. A. Baldo, M. E. Thompson and S. R. Forrest, *J. Appl. Phys.*, 2001, **90**, 5048–5051.
- 3 Y. Tao, C. Yang and J. Qin, *Chem. Soc. Rev.*, 2011, **40**, 2943–2970.
- 4 S. Reineke, G. Schwartz, K. Walzer and K. Leo, *Appl. Phys. Lett.*, 2007, **91**, 123508.
- 5 M. Romain, D. Tondelier, B. Geffroy, A. Shirinskaya, O. Jeannin, J. Rault-Berthelot and C. Poriel, *Chem. Commun.*, 2015, **51**, 1313–1315.
- 6 L. Ding, S.-C. Dong, Z.-Q. Jiang, H. Chen and L.-S. Liao, *Adv. Funct. Mater.*, 2015, **25**, 645–650.
- 7 K. Nasu, T. Nakagawa, H. Nomura, C.-J. Lin, C.-H. Cheng, M.-R. Tseng, T. Yasuda and C. Adachi, *Chem. Commun.*, 2013, **49**, 10385–10387.
- 8 B. Pan, B. Wang, Y. Wang, P. Xu, L. Wang, J. Chen and D. Ma, *J. Mater. Chem. C*, 2014, **2**, 2466–2469.
- 9 Y. Zhao, C. Wu, P. Qiu, X. Li, Q. Wang, J. Chen and D. Ma, *ACS Appl. Mater. Interfaces*, 2016, **8**, 2635–2643.
- 10 Y.-K. Wang, Q. Sun, S.-F. Wu, Y. Yuan, Q. Li, Z.-Q. Jiang, M.-K. Fung and L.-S. Liao, *Adv. Funct. Mater.*, 2016, **26**, 7929–7936.
- 11 S. Thiery, D. Tondelier, B. Geffroy, O. Jeannin, J. Rault-Berthelot and C. Poriel, *Chem. – Eur. J.*, 2016, **22**, 10136–10149.
- 12 J. Rosevear and J. F. K. Wilshire, *Aust. J. Chem.*, 1991, **44**, 1097–1114.
- 13 Y. Hirota, *J. Mater. Chem.*, 2000, **10**, 1–25.
- 14 Z. Ge, T. Hayakawa, S. Ando, M. Ueda, T. Akiike, H. Miyamoto, T. Kajita and M. Kakimoto, *Adv. Funct. Mater.*, 2008, **18**, 584–590.
- 15 Y. Tao, Q. Wang, L. Ao, C. Zhong, J. Qin, C. Yang and D. Ma, *J. Mater. Chem.*, 2010, **20**, 1759–1765.
- 16 B. M. Bell, T. P. Clark, T. S. De Vries, Y. Lai, D. S. Laitar, T. J. Gallagher, J.-H. Jeon, K. L. Kearns, T. McIntire, S. Mukhopadhyay, H.-Y. Na, T. D. Paine and A. A. Rachford, *Dyes Pigments*, 2017, **141**, 83–92.
- 17 D. Zhao, J. Hu, N. Wu, X. Huang, X. Qin, J. Lan and J. You, *Org. Lett.*, 2011, **13**, 6516–6519.
- 18 Y. Watanabe, H. Sasabe, D. Yokoyama, T. Beppu, H. Katagiri, Y.-J. Pu and J. Kido, *Adv. Opt. Mater.*, 2015, **3**, 769–773.
- 19 F. Kessler, Y. Watanabe, H. Sasabe, H. Katagiri, M. K. Nazeeruddin, M. Grätzel and J. Kido, *J. Mater. Chem. C*, 2013, **1**, 1070–1075.
- 20 S. Gong, Y.-L. Chang, K. Wu, R. White, Z.-H. Lu, D. Song and C. Yang, *Chem. Mater.*, 2014, **26**, 1463–1470.
- 21 H. Shin, S. Lee, K.-H. Kim, C.-K. Moon, S.-J. Yoo, J.-H. Lee and J.-J. Kim, *Adv. Mater.*, 2014, **26**, 4730–4734.
- 22 C. Fan, L. Zhu, T. Liu, B. Jiang, D. Ma, J. Qin and C. Yang, *Angew. Chem. Int. Ed.*, 2014, **53**, 2147–2151.
- 23 J.-G. Yang, L.-Z. Xu, L. Huang, J.-R. Gao, M.-C. Liu, F.-Y. Pan and D.-B. Chen, *Chin. Chem. Lett.*, 2016, **27**, 340–344. [View Article Online](#) DOI: 10.1039/C6CC00903A